

3T BODY MRI

Neil M. Rofsky, MD

nrofsky@bidmc.harvard.edu

Beth Israel Deaconess Med Center / Harvard Med School, Boston, MA, US

INTRODUCTION

The inherent doubling in signal-to-noise ratio when compared to 1.5T provides unique opportunities for body MR imaging at 3T. The augmented SNR can be used to improve anatomic and/or temporal resolution and reduce breath hold time periods while preserving image quality. However, susceptibility, and chemical shift dispersion are also increased at 3.0T (scaling with field strength) and T1 and T2 are increased. These features impose challenges for certain aspects of body imaging. Our preliminary experience with body imaging at 3.0T shows excellent results for fMRI spectroscopy sensitivity, and MRA conspicuity. The development of a whole body transmit/receive RF coil, (1) is the fundamental achievement enabling whole body aiming at 3.0T. This has allowed for the evaluation beyond a clinical head-only scanner (2) into a clinical whole-body scanner.

HIGHER SIGNAL TO NOISE - IMAGING

The higher the field strength, the more protons (or other nuclei of interest) are aligned with the main magnetic field. Thus there are more protons (or other nuclei) available to participate in and provide signal for the MR experiment. Signal to noise (SNR) varies linearly with field strength and is therefore twice as high at 3T than at 1.5 T.

Higher signal to noise can be exploited in different ways: (a) to image at higher spatial resolution (i.e. smaller field of view, higher matrix and/or thinner slices) or (b) to image more rapidly, at comparable levels of spatial resolution or (c) a combination of both.

Imaging at higher spatial resolution allows one to visualize smaller structures with improved detail or to improve the detection rate of smaller details vulnerable partial volume effects.

POWER DEPOSITION

The amount of radiofrequency energy needed to displace the proton away from its alignment with the main magnetic field, into the transverse plane varies proportionately with the strength of the main magnetic field. Thus to achieve a given sequence at higher field strength, more energy must be deposited – this results in an increase in the specific absorption rate (SAR).

SAR is a measure of the amount of energy deposited by an RF field in a given mass of tissue, measured in watts per kilogram (W/kg). For a sphere of homogeneous tissue, both the average and peak SAR are proportional to the main magnetic field and to the square of the RF flip angle, as follows:

$$\text{SAR} \propto \mathbf{B}_0^2 \sigma r^2 \alpha^2 D$$

where B_0 is the main magnetic field, σ is conductivity of the tissue, r is the radius of the sphere of tissue, α is the RF flip angle, and D is the duty cycle of the sequence. Thus, at 3T, SAR effects are approximately 4X those at 1.5T. SAR limits are set by governing agencies. In the U.S.A. the FDA guidelines require that SAR levels do not exceed 4 W/kg (whole body, averaged over 15 minutes) or 8 W/kg (in any gram of tissue in the head or torso, for any 5 minute period) (see www.fda.gov/cdrh/ode/magdev.html).

The MR manufacturers configure scanners to function within the guidelines of the relevant governing bodies. A power monitor may be provided to allow real-time monitoring of power characteristics. The presence of built-in safeguards can interfere with routine imaging, by limiting the performance of the system (e.g. limiting the number of sections that can be acquired per unit time).

SAR-intensive sequences tend to be those which employ multiple 180° refocusing pulses, such as fast spin echo, STIR, FLAIR sequences as well as GRE sequences with very short TRs, which entail a high duty cycle (e.g. True FISP or FIESTA). Strategies to minimize power deposition and avoid encountering SAR limitations include: use of partial flip angles (e.g. 150° instead of 180°) in fast spin echo sequences (3), use of shorter echo train lengths and increased echo spacing in fast spin echo sequences, incorporating dead times into a sequence, use of lower (for a given TR) flip angles in GRE imaging, avoidance of short TE sequences, and use of specialized RF pulses that deliver energy over a longer period of time (e.g. adiabatic pulses). However, many of these strategies result in an increased scan time. As previously mentioned parallel imaging offers a reduction in Rf/unit time. In order to maximize the performance of our 3T system and to improve throughput, we routinely run the system at the highest permissible SAR levels.

DECREASED RF (B1) FIELD HOMOGENEITY

Difficulties related to radiofrequency (RF) field homogeneity represent another challenge to clinical imaging at 3T (4). Two factors lead to decreased RF field homogeneity at high field strength (5). One factor is shorter penetration distance or “skin depth” of RF into the sample, because of electrical conductivity. At higher frequencies, RF is dissipated to a greater degree as it passes through the tissues. Based on this, the field should become weaker at the center of the sample. The second factor affecting field homogeneity is the increase in dielectric constants of water and tissue at high field and its effect of shortening the wavelength of RF in the sample. The wavelength of RF at 3T is such that it sets up a resonant cavity or “waveguide” effect within the sample, with the result that the amplitude or phase of the RF varies with position inside the sample. This spatial variation of RF results in center brightening of the image. These two effects have potential to counterbalance each other, but not necessarily in a uniform manner. To cope with the issues of RF penetrance and dielectric constant alternate RF pulse designs (e.g. adiabatic pulses), pulse sequence designs (e.g. phase cycling), and coil designs are being pursued in order to maximize the imaging at 3T.

COILS

While the body coil results are quite impressive, the development of localized coils still is an important part of optimizing the 3.0T platform. Preliminary data suggests that phased array coil imaging of the prostate can match the image quality achieved with the endorectal coil at 1.5T (6). This provides flexibility for patients who cannot tolerate the endorectal coil. On the other hand the opportunity for higher resolution and/or reduced scan times can be further exploited with an endorectal coil at 3T (7, 8). Recent results suggest an improved accuracy in staging achieved at 3T with an ERC (9).

The use of localized coils dovetails with the pursuit of parallel imaging at 3.0T, where SNR 'headroom' allows for similar image quality as that achievable at 1.5T with a phased array coil but in $\frac{1}{2}$ the acquisition time. Preserved SNR with reduced acquisition time allows for a greater capture rate of diagnostic imaging in those patients with limited breath hold capacity.

PARALLEL IMAGING

Parallel imaging is a technique that considerably reduces scan time. Spatial information garnered from coils of a receiver array is used for reducing conventional Fourier encoding. There is a particularly promising synergy between high field and parallel imaging. On the one hand, parallel imaging may be used to address many of the technical difficulties associated with high field strengths. For example, SAR can be reduced by decreasing the RF duty cycle, and the vulnerability to field inhomogeneity (e.g. for EPI and spiral techniques) can be reduced by shortening acquisition times.

High field strength extends the ultimate capabilities of parallel imaging. Acceleration in parallel MRI comes at a cost in SNR – the higher the acceleration, the greater the SNR penalty. The inherent SNR advantage at 3T (resulting from increased spin polarization) allows for greater acceleration factors and/or higher degrees of resolution to be pursued while maintaining image quality. Moreover, recent theoretical investigations (10, 11) at our center and elsewhere have predicted that the combination of high field strength and parallel imaging will afford SNR advantages above and beyond those resulting from increased spin polarization. In particular, the increased ability to focus radiofrequency energy at high RF frequencies has been shown to result in an improved capacity for spatial encoding with coil arrays, and hence in higher SNR and higher achievable accelerations for high-field parallel imaging.

From a patient safety perspective are the concerns regarding current densities and the rates of RF energy power deposition (specific absorption rates or SARs) in various organs. A potential constraint for routine clinical imaging is RF heating, since SAR is four times as large at 3.0 T as at 1.5 T.

T1 and T2 Changes at 3T

T1 relaxation time, also known as longitudinal or spin-lattice relaxation time, is a property of a proton (or other relevant nucleus) within a given molecular environment, and is dependent on B_0 , the main magnetic field (12).

We recently used a half-Fourier acquisition single shot fast spin echo sequence combined with inversion recovery and multiple spin-echo preparation to measure the T1 and T2 of abdominal and pelvic tissues within a breath hold (13). Accurate relaxation time measurements of T1 and T2 at 1.5 and 3.0 Tesla were obtained for liver, spleen, kidney, pancreas, bone marrow, fat, prostate, and uterus. The longer T1 values in tissues at 3T was confirmed. For imaging, the field strength dependence on relaxation rates has an important bearing on the choice of pulse sequence and image contrast.

The longer T1 values can prolong the magnetic 'tag' of labeled blood in arterial spin labeling. Initial work is exploring this capacity to extend the functional assessments of renal perfusion (14) and quantifying blood flow in patients with renal cell carcinoma. The technique may be useful for evaluating tumor response to antiangiogenic agents response of renal cell carcinoma to antiangiogenesis agents (15).

T2 RELAXATION TIME

T2 relaxation time, also known as transverse or spin-spin relaxation time, is a property which reflects a particular local microscopic environment. Although it is subject to B_0 effects, in fact, T2 values are typically unchanged or only slightly decreased with increases in field strength. This is because some mechanisms of T2 relaxation are prolonged with increased field strength, while others become more efficient.

T2 and SUSCEPTIBILITY*

Magnetic susceptibility can be thought of as a material's tendency to distort an applied field. The net induced magnetization is typically proportional to the applied field. Variations in magnetic susceptibilities within a voxel such as those at air-tissue interfaces produce local inhomogeneities in the magnetic field. These field inhomogeneities produce dephasing which results in T2* signal loss and such losses are prominent when GRE sequences are being employed. A real concern is the artifacts that can be induced at air-soft tissue interfaces and adjacent to metallic surgical clips and indwelling metallic stents. On the other hand the opportunity to improve sensitivity to the detection of hemorrhage can be realized and greater sensitivity to blood oxygenation level dependent (BOLD) contrast.

CONTRAST MEDIA

The increase in T1 and susceptibility seen at 3T has important implications for the optimal use of contrast agents. Agents facilitating T1 relaxation (e.g. Gd-chelates) can have a more dramatic contrast effect due to the relative lower signal of background tissues resulting from the prolonged T1 of tissues at 3T vs. 1.5T. The relaxivity of

gadolinium actually decreases slightly with field strength (16). However, the T1 relaxation values of the various body tissues lengthen with increased field strength, so the impact of the gadolinium can be more pronounced. We have noticed an increased sensitivity to the concurrent T2* shortening that effects Gd at 3T and in our preliminary assessments, rapid bolus imaging can be contaminated by a confounding T2* effect. This has resulted in our group's effort to better understand the trade-offs of dose/rate and imaging parameters for tumor perfusion imaging and for the optimization of MR angiography. The susceptibility sensitivity has implications for then use of SPIO agents and other agents that can augment the T2* relaxation. Optimal administration schemes need to be established while considering the prospect for improved liver:lesion contrast-to-noise at 3T.

CHEMICAL SHIFT

The local chemical environment, that is the structure of the specific molecule, can subtly modify the resonance frequency of a nucleus and result in a shift in the nuclear resonance frequency. There are two sources of the frequency shift: 1) the electron cloud surrounding a nucleus shields it from the applied static (B_0) field causing it to experience a lower effective B_0 field; and 2) neighboring atoms and groups attached to the molecule give rise to magnetic moments that change the local field that the nucleus experiences. The difference between a proton in a water molecule and one on a CH₂ group is ~ 3.5 ppm and this is quite applicable to imaging and artifact considerations from fat and water protons. At 1.5T (64MHz) the chemical shift is 224Hz whereas at 3.0T it is 448 Hz. This can result in more severe chemical shift artifacts at fat-soft tissue interfaces, particularly with lower bandwidth imaging. On the other hand the ability to image or suppress one of these moieties is facilitated at the higher field strength. Furthermore, the entire field of MR spectroscopy benefits from a synergistic effect between the improved spectral resolution from chemical shift effects and the augmented SNR.

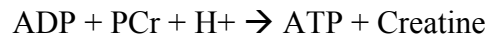
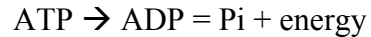
HIGHER SIGNAL TO NOISE – PROTON SPECTROSCOPY

Higher SNR facilitates proton spectroscopy and spectroscopic imaging, particularly in cases where assessment has been limited by small concentrations and long measurement times. Because of higher SNR, the amplitude of a peak for a given chemical species should, in theory, be larger at 3T than at 1.5T. In addition, when SNR is higher, measurement times for acquiring sufficient data for analysis can be reduced. This can be especially advantageous for in vivo applications where data acquisition times are constrained by gross and physiologic patient motion.

HIGHER SIGNAL TO NOISE – NUCLEI OTHER THAN PROTONS

Although most clinical MR is based on evaluation of the proton nucleus, several other nuclei are amenable to MR evaluation, including ²³Na and ³¹P. The inherently low concentrations of those moieties necessitate very long imaging times at 1.5 Tesla that are not clinically feasible. At higher field strengths, spectroscopy as well as imaging based on these alternative nuclei becomes feasible. Sodium MR offers a tool for assessing

shifts in the balance of intra- and extra-cellular water associated with various pathologic states. In addition, sodium has been found to accumulate preferentially in intra-substance foci of cartilage degeneration, providing a measure of early cartilage degradation (17). Detection of sodium may also form the basis for “functional” imaging of cartilage, by demonstrating differential decreases in sodium content following mechanical compression. ^{31}P is another paramagnetic species that is reasonably abundant in vivo, but clearly benefits from the higher SNR available at 3T. ^{31}P plays a central role in energy metabolism. Inorganic phosphate (Pi) is a breakdown product of ATP metabolism, while phosphocreatine (PCr) must be present to generate new stores of ATP.



Separate peaks for Pi and PCr as well as from the different phosphorus nuclei on the ATP molecule can be resolved and quantitated. The ratio of Pi/PCr provides a useful measure of tissue energetics in vivo (18). For example, increased Pi/PCr has been observed in resting muscle of patients suffering from peripheral vascular disease. Pi/PCr appears to correlate with the extent of ischemia, as it is higher in pts with rest pain and even higher in pts with gangrene or ulceration. Greater depletion of PCr during exercise and slower recovery to equilibrium values in patients with severe ischemia, compared with normals, has also been reported. While both ^{23}Na and ^{31}P can be imaged at 1.5 Tesla with the appropriate coils and software adjustments (and indeed much of the early in vivo work on these nuclei was performed at 1.5T), the higher SNR available at 3T allows for more robust measurement and, too, facilitates direct imaging of these metabolites – i.e. sodium images or Pi and PCr images -- at a useful level of spatial resolution. Initial data is demonstrating potential clinical benefit in assessing early stage diabetic foot problems and in elucidating mechanisms of disease (19, 20).

CONCLUSIONS

In vivo MRI/MRS at 3 Tesla provides a number of promising opportunities for clinical assessment. High field strength at 3T provides increased SNR for routine proton imaging. Increased SNR can be invested in higher spatial or temporal resolution. Increased SNR also facilitates spectroscopy and imaging of less abundant species providing new opportunities for evaluating sodium distribution and tissue energetics, assessments that are difficult to evaluate at lower field. Sequences can be optimized at 3T to account for changes in T1 relaxation times and behavior of gadolinium contrast. Strategies exist for addressing increased energy deposition and increased chemical shift and susceptibility artifacts. Fundamental differences in the behavior of RF fields at 3T necessitate a critical assessment of RF pulses, pulse sequence structures, and coil designs.

REFERENCES

1. Watkins et al. ISMRM9. 2001:1123.
2. Hugg et al. ISMRM9. 2001:1349.

3. Alsop DC. The sensitivity of low flip angle RARE imaging. *Magn Reson Med* 1997;37(2):176-184.
4. Greenman RL, Shirosky JE, Mulkern RV, Rofsky NM. Double inversion black-blood fast spin-echo imaging of the human heart: a comparison between 1.5T and 3.0T. *J Magn Reson Imaging* 2003;17(6):648-655.
5. Ugurbil K, Garwood M, Ellermann J, Hendrich K, Hinke R, Hu X, et al. Imaging at high magnetic fields: initial experiences at 4 T. *Magn Reson Q* 1993;9(4):259-277.
6. Sosna J, Pedrosa I, Dewolf WC, Mahallati H, Lenkinski RE, Rofsky NM. MR imaging of the prostate at 3 Tesla: comparison of an external phased-array coil to imaging with an endorectal coil at 1.5 Tesla. *Acad Radiol* 2004;11(8):857-862.
7. Futterer JJ, Scheenen TW, Huisman HJ, Klomp DW, van Dorsten FA, Hulsbergen-van de Kaa CA, et al. Initial Experience of 3 Tesla Endorectal Coil Magnetic Resonance Imaging and 1H-Spectroscopic Imaging of the Prostate. *Invest Radiol* 2004;39(11):671-680.
8. Bloch BN, Rofsky NM, Baroni RH, Marquis RP, Pedrosa I, Lenkinski RE. 3 Tesla magnetic resonance imaging of the prostate with combined pelvic phased-array and endorectal coils; Initial experience(1). *Acad Radiol* 2004;11(8):863-867.
9. Futterer JJ, Heijmink SW, Scheenen TW, Jager GJ, Hulsbergen-Van de Kaa CA, Witjes JA, et al. Prostate cancer: local staging at 3-T endorectal MR imaging--early experience. *Radiology* 2006;238(1):184-191.
10. Ohliger M, Yeh E, McKenzie C, Sodickson D. Constraints on the Performance of Parallel Magnetic Resonance Imaging. *Scientific Meeting of the International Society for Magnetic Resonance in Medicine*. Honolulu, HI, USA 2002:2387.
11. Wiesinger F, Pruessmann K, Boesiger P. Inherent Limitation of the Reduction Factor in Parallel Imaging as a Function of Field Strength. *Tenth Scientific Meeting of the International Society for Magnetic Resonance in Medicine*. Honolulu, HI, USA, 2002:191.
12. Koenig SH, Brown RD, 3rd. Relaxation of solvent protons by paramagnetic ions and its dependence on magnetic field and chemical environment: implications for NMR imaging. *Magn Reson Med* 1984;1(4):478-495.
13. de Bazelaire CM, Duhamel GD, Rofsky NM, Alsop DC. MR imaging relaxation times of abdominal and pelvic tissues measured in vivo at 3.0 T: preliminary results. *Radiology* 2004;230(3):652-659.
14. Boss A, Martirosian P, Graf H, Claussen CD, Schlemmer HP, Schick F. High resolution MR perfusion imaging of the kidneys at 3 Tesla without administration of contrast media. *Rofo* 2005;177(12):1625-1630.
15. De Bazelaire C, Rofsky NM, Duhamel G, Michaelson MD, George D, Alsop DC. Arterial spin labeling blood flow magnetic resonance imaging for the characterization of metastatic renal cell carcinoma(1). *Acad Radiol* 2005;12(3):347-357.
16. Bernstein MA, Huston J, Lin C, Gibbs GF, Felmlee JP. High-resolution intracranial and cervical MRA at 3.0T: Technical considerations and initial experience. *Magn Reson Med* 2001;46(5):955-962.
17. Shapiro EM, Borthakur A, Dandora R, Kriss A, Leigh JS, Reddy R. Sodium visibility and quantitation in intact bovine articular cartilage using high field (23)Na MRI and MRS. *J Magn Reson* 2000;142(1):24-31.

18. Greenman RL, Axel L, Ferrari VA, Lenkinski RE. Fast imaging of phosphocreatine in the normal human myocardium using a three-dimensional RARE pulse sequence at 4 Tesla. *J Magn Reson Imaging* 2002;15(4):467-472.
19. Greenman RL, Khaodhiar L, Lima C, Dinh T, Giurini JM, Veves A. Foot small muscle atrophy is present before the detection of clinical neuropathy. *Diabetes Care* 2005;28(6):1425-1430.
20. Greenman RL, Panasyuk S, Wang X, Lyons TE, Dinh T, Longoria L, et al. Early changes in the skin microcirculation and muscle metabolism of the diabetic foot. *Lancet* 2005;366(9498):1711-1717.

NOTES

